Supplemental Material for

Systems analysis of guard cell membrane transport for enhanced stomatal dynamics and water use efficiency

Yizhou Wang, Adrian Hills and Michael R. Blatt

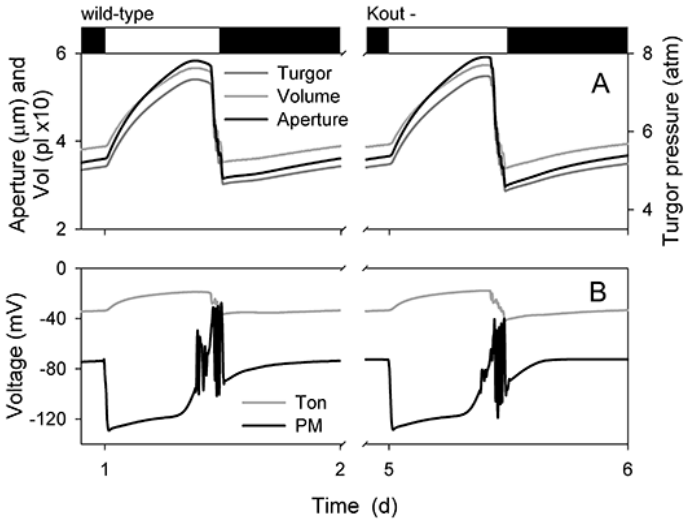

Fig. S1. Macrosocpic ouputs from the OnGuard model. Outputs resolved over a standard diurnal cycle (12 h light:12 h dark, indicated by bars above) with 10 mM KCl, 1 mM $CaCl_2$ and pH 6.5 outside (Chen et al. 2012). Representative diurnal cycles are shown for the wild-type (control, *left*) and Kout- manipulation (*right*), equivalent to a -18 mV shift in the mid-point voltage for GORK channel gating in Arabidopsis. For the results in this and the subsequent figures, the simulation was initiated with wild-type parameters (Wang et al. 2012) and the Kout- component current manipulated at the start of day 3, yielding a new stable cycle from day 4 onwards. A summary analysis is provided with each of the subsequent figures; further details will be found in Chen, et al. (2012). Shown are (A) stomatal aperture, turgor pressure and total guard cell volume, and (B) plasma membrane and tonoplast voltages. Stomatal apertures varied over a physiological range between roughly 3 µm and 6 µm in the wild-type and were parallelled by physiologically sensible changes in guard cell volume and turgor. Following stomatal closure at the end of the day, the model generated a small and gradual rise in aperture and the associated outputs that anticipated the start of the next day, much as has been observed in vivo (Gorton et al. 1993; Meidner and Willmer 1993). The start of the day was associated with hyperpolarisation of the plasma membrane to voltages near -130 mV and the dark period was marked by depolarisation of the plasma membrane to voltages near the equilibrium voltage for K^+, consistent with the diurnal cycle in energetic outputs of the ATP-driven pumps (Raschke 1979; Spanswick 1981; Blatt 1987; McClure et al. 1989; Blatt and Clint 1989; Clint and Blatt 1989; Kinoshita et al. 1995). Voltage oscillations at the end of the daylight period are detailed by Chen, et al. (2012) and mark periods of substantial K^+ and anion efflux that drive stomatal closure. These oscillations arise from coordinated oscillations in elevated $[Ca^{2+}]_i$ and enhanced K^+ and anion channel activity (see Supplemental Figs. S2, S4 and S6).

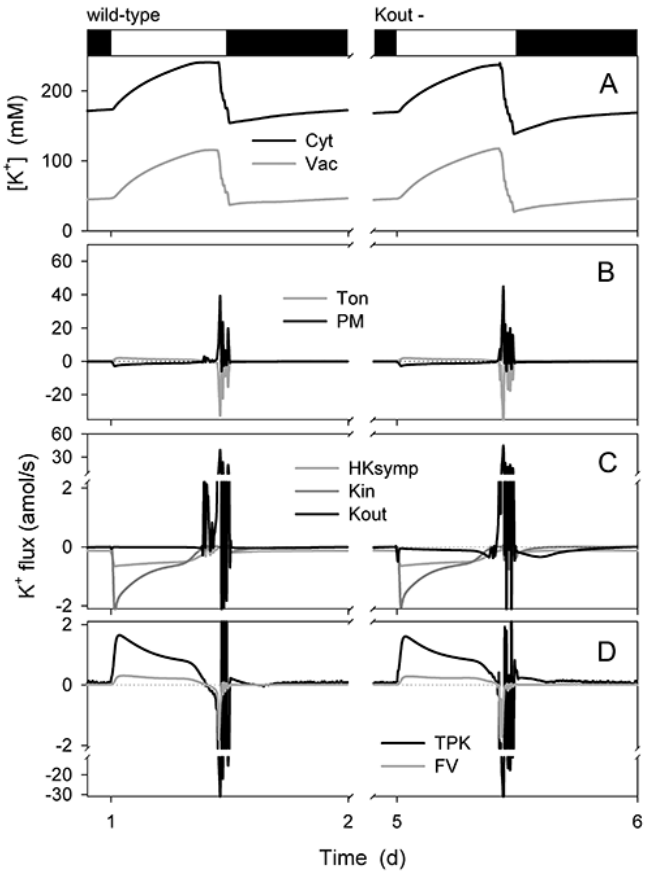

Fig. S2. K^+ contents and analysis of K^+ fluxes at the plasma membrane (PM) and tonoplast (Ton). Outputs resolved over a standard diurnal cycle (12 h light:12 h dark, indicated by bars above) (Chen et al. 2012) for the wild-type (control, *left*) and Kout- manipulation (*right*) as described in Supplemental Fig. S1. Shown are (A) cytosolic and vacuolar [K^+], (B) the net K^+ flux across the plasma membrane and tonoplast, (C) the K^+ flux through the K^+-permeable transporters at the plasma membrane, comprising the two K^+ channels and the H^+-K^+ symporter, and (D) the K^+ flux through the K^+ permeable transporters at the tonoplast, comprising the TPK and FV channels. K^+ flux through the TPC channel accounted for less than one percent of either of the other channel fluxes, and has therefore been omitted for purposes of clarity. Positive flux is defined as movement of the ionic species (not the charge) out of the cytosol, either across the plasma membrane or the tonoplast. Note that the bulk of K^+ entering across the plasma membrane is shunted across the tonoplast to the vacuole during the day and this pattern reversed in the first hours of dark, as expected from experimental observation (Hills et al. 2012; Chen et al. 2012). At the plasma membrane (C), K^+ influx was dominated by $I_{K,in}$ in the first half of the day, and roughly matched by flux through the H^+-K^+ symport in the second half of the day. Closure was marked by the predominance of K^+ efflux through Kout which relaxed to a near-zero value during the night. These simulations show a minor influx through Kout at the end of the daylight period when manipulated to open at the more negative voltages. This additional influx accounts in part for the small elevation in aperture maximum (Fig. S1), but has no substantial effect otherwise. Modifying Kout facilitates oscillations and K^+ efflux at the end of the daylight period and leads to a small decrease in the minimum aperture and acceleration of initial reopening in the dark.

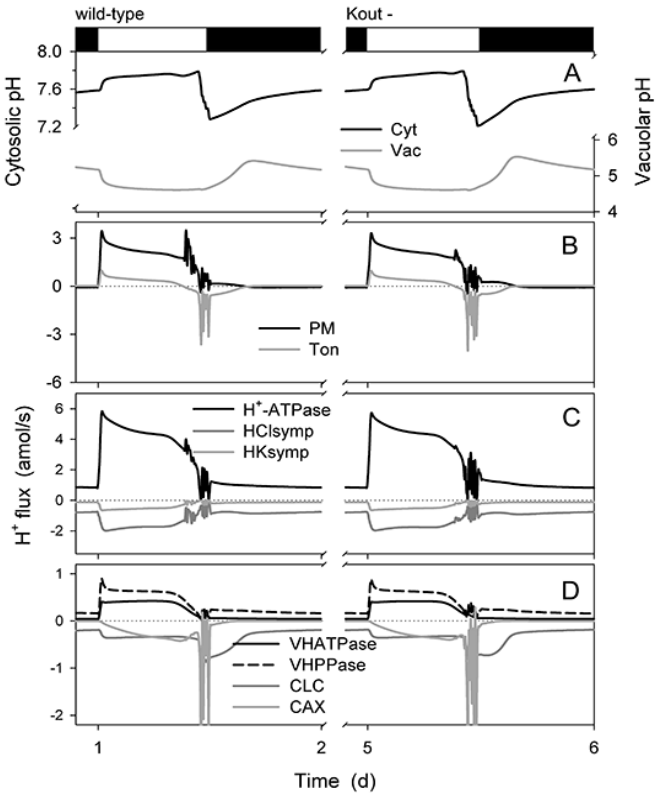

Fig. S3.Cytosolic and vacuolar pH, and H^+ fluxes across the plasma membrane and tonoplast. Outputs resolved over a standard diurnal cycle (12 h light:12 h dark, indicated by bars above) (Chen et al. 2012) for the wild-type (control, *left*) and Kout- manipulation (*right*) as described in Supplemental Fig. S1. Shown are (A) cytosolic and vacuolar pH, (B) the net H^+ flux across the plasma membrane and tonoplast, (C) the H^+ flux through the H^+-permeable transporters at the plasma membrane, comprising the H^+-ATPase, and the H^+-K^+ and H^+-Cl^- symporters, and (D) the H^+ flux through the H^+ permeable transporters at the tonoplast, comprising the VH^+-ATPase, VH^+-PPase, the CLC H^+-Cl^- antiporter and the CAX H^+-Ca^{2+} antiporter. Positive flux is defined as movement of the ionic species (not the charge) out of the cytosol, either across the plasma membrane or the tonoplast. The bulk of H^+ production associated with daytime Mal synthesis (Supplemental Fig. S5) is exported via the plasma membrane H^+-ATPase, with roughly 20% transported to the vacuole (B-D). In the vacuole, Mal comprises the major pH buffer and its accumulation is associated with acidification of the vacuolar contents (Van Kirk and Raschke 1978; Outlaw 1990; Talbott and Zeiger 1993; Willmer and Fricker 1996). Diurnal changes in vacuolar pH in the model resulted primarily from Mal transport and charge balance with H^+ (Supplemental Fig. S5). The organic acid is thought to be transported as the fully deprotonated (Mal^{2-}) form – with the ALMT channel as the primary pathway for tonoplast Mal^{2-} flux [reviewed by Hills, et al. (Hills et al. 2012)] – implying charge balance via the tonoplast VH^+-ATPase and H^+-PPase (Rea and Poole 1993; Martinoia et al. 2007). Minor effects of the modification of Kout gating are visible in depression of cytosolic pH at the end of the daylight period and arise from a small change in H^+ fluxes at this time, mainly through the H^+-ATPase and CLC H^+-Cl^- antiporter.

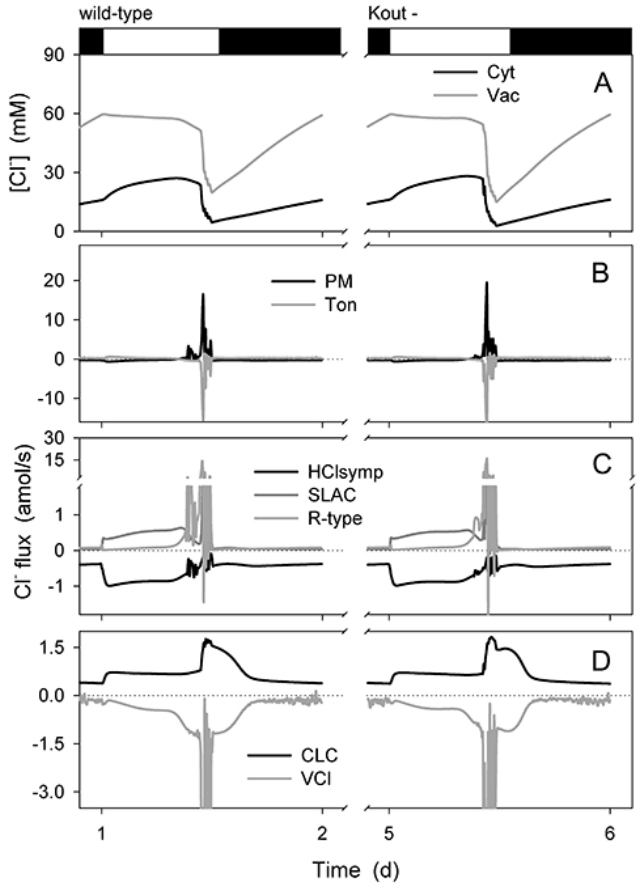

Fig. S4. Chloride contents and analysis of Cl^- fluxes at the plasma membrane and tonoplast. Outputs resolved over a standard diurnal cycle (12 h light:12 h dark, indicated by bars above) (Chen et al. 2012) for the wild-type (control, *left*) and Kout- manipulation (*right*) as described in Supplemental Fig. S1. Shown are (A) total cytosolic and vacuolar [Cl^-], (B) the net flux of Cl^- across the plasma membrane and tonoplast, (C) the flux of Cl^- through the Cl^--permeable transporters at the plasma membrane, comprising the SLAC and R-type anion channels and H^+-Cl^- symporter, and (D) the flux of Cl^- through the Cl^--permeable transporters at the tonoplast, comprising the VCl channel and CLC H^+-Cl^- antiporter. Positive flux is defined as movement of the ionic species (not the charge) out of the cytosol, either across the plasma membrane or the tonoplast. Note the expanded scales in (C) and (D). Both wild-type and Kout- modifications yield cytosolic and vacuolar Cl^- concentrations that exhibit complex, biphasic responses to the diurnal cycle, in effect leading to an exchange of Cl^- for Mal accumulated in the daytime and vice versa at night (compare Supplemental Fig. S5) (Raschke and Schnabl 1978; Talbott and Zeiger 1993; Talbott and Zeiger 1996). Stomatal opening was accompanied by a net efflux of Cl^- from the vacuole to the cytosol and, later in the daylight period from the cytosol to the apoplast. Closure was marked by much larger fluxes of Cl^- from the vacuole to the cytosol and export across the plasma membrane; this pattern reversed after the first 1-2 h of dark. The rise in cytosolic Cl^- concentration during the first hours of the day arose from the rapid Cl^- influx across the tonoplast and a slower rise in the rate of Cl^- export across the plasma membrane. Modifying Kout gating leads only to an enhanced efflux at the plasma membrane and, at the tonoplast, through the CLC antiporter at the end of the daylight period.

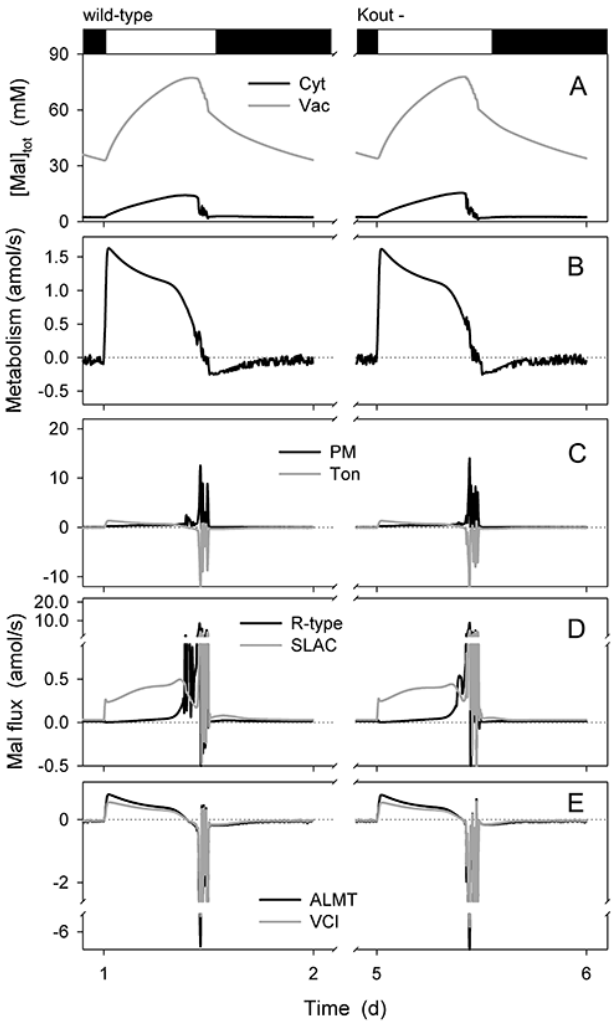

Fig. S5. Malic acid synthesis, total malate (Mal) contents and analysis of Mal^{2-} fluxes at the plasma membrane and tonoplast. Outputs resolved over a standard diurnal cycle (12 h light:12 h dark, indicated by bars above) (Chen et al. 2012) for the wild-type (control, *left*) and Kout- manipulation (*right*) as described in Supplemental Fig. S1. Shown are (A) total cytosolic and vacuolar [Mal], (B) the rates of Mal synthesis and metabolism, (C) the net flux of Mal^{2-} across the plasma membrane and tonoplast, (D) the Mal^{2-} flux through the Mal^{2-}-permeable transporters at the plasma membrane, comprising the SLAC and R-type anion channels, and (E) the Mal^{2-} flux through the Mal^{2-} permeable transporters at the tonoplast, comprising the ALMT and VCl channels. Positive flux is defined as movement of the ionic species (not the charge) out of the cytosol, either across the plasma membrane or the tonoplast. These simulations, show no substantial effect modifying Kout gating. In both cases, the bulk of Mal production was diverted by transport of Mal^{2-} across the tonoplast, leading to a rise in total vacuolar Mal from 30 mM at the end of the night to near 90 mM before declining at the end of the daylight period; Mal in the cytosol rose from approximately 1 mM to values near 15 mM, much as estimated from experimental data and summarised previously (Hills et al. 2012). Mal efflux at the plasma membrane is predicted to be mediated largely by the SLAC-type anion channel during daylight with the added contribution of flux through the R-type anion channel during stomatal closure.

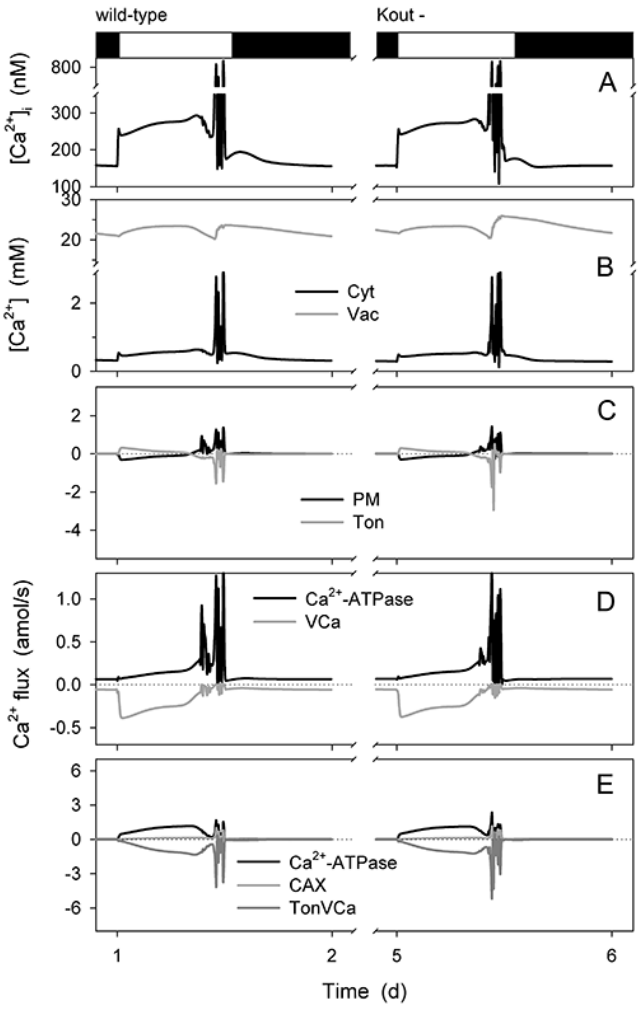

Fig. S6. Cytosolic and vacuolar [Ca^{2+}], cytosolic-free [Ca^{2+}] ([Ca^{2+}]$_i$), and analysis of Ca^{2+} fluxes across the plasma membrane and tonoplast. Outputs resolved over a standard diurnal cycle (12 h light:12 h dark, indicated by bars above) (Chen et al. 2012) for the wild-type (control, *left*) and Kout-manipulation (*right*) as described in Supplemental Fig. S1. Shown are (A) the cytosolic-free [Ca^{2+}], (B) the total [Ca^{2+}], (C) the net flux of Ca^{2+} across the plasma membrane and tonoplast, (D) the Ca^{2+} flux through the Ca^{2+}-permeable transporters at the plasma membrane, comprising the hyperpolarisation-activated Ca^{2+} channel VCa and the Ca^{2+}-ATPase, and (E) the flux of Ca^{2+} through the Ca^{2+}-permeable transporters at the tonoplast, comprising the Ca^{2+}-ATPase, the CAX H^+-Ca^{2+} antiporter, and the TonVCa Ca^{2+} channel. Flux through the TPC channel accounts for less than two percent of the total Ca^{2+} flux across the tonoplast and has therefore been omitted for purposes of clarity. Positive flux is defined as movement of the ionic species (not the charge) out of the cytosol, either across the plasma membrane or the tonoplast. Both in wild-type and modified Kout simulations[Ca^{2+}]$_i$ is predicted to rise from a resting value near 160 nM in the dark to a mean daylight value near 260 nM (A). Stomatal closure is accompanied by a series of voltage (Supplemental Fig. S1) and [Ca^{2+}]$_i$ oscillations that drive K^+ and anion efflux during closure (Gilroy et al. 1991; Thiel et al. 1992; Irving et al. 1992; McAinsh et al. 1992; Blatt and Armstrong 1993; Gradmann et al. 1993; Grabov and Blatt 1998; Staxen et al. 1999). Further details will be found in Chen, et al. (Chen et al. 2012). Vacuolar Ca^{2+} circulation dominates over transport at the plasma membrane by at least one order of magnitude (Sanders et al. 2002; Blatt et al. 2007; McAinsh and Pittman 2009) and is essential to potentiating [Ca^{2+}]$_i$ signals (Gilroy et al. 1991; McAinsh et al. 1991; Grabov and Blatt 1997; Grabov and Blatt 1998; Grabov and Blatt 1999; Garcia-Mata et al. 2003). Again, these results show no substantial difference between the two simulations.

References:

1. Blatt MR (1987) Electrical characteristics of stomatal guard cells: the ionic basis of the membrane potential and the consequence of potassium chloride leakage from microelectrodes. Planta 170: 272-287

2. Blatt MR, Armstrong F (1993) K^+ channels of stomatal guard cells: abscisic acid-evoked control of the outward rectifier mediated by cytoplasmic pH. Planta 191: 330-341

3. Blatt MR, Clint GM (1989) Mechanisms of fusicoccin action kinetic modification and inactivation of potassium channels in guard cells. Planta 178: 509-523

4. Blatt MR, Garcia-Mata C, Sokolovski S (2007) Membrane transport and Ca^{2+} oscillations in guard cells. In S Mancuso, S Shabala, eds, Rhythms in Plants, Ed 1. Springer, Berlin, pp 115-134

5. Chen ZH, Hills A, Baetz U, Amtmann A, Lew VL, Blatt MR (2012) Systems Dynamic Modeling of the Stomatal Guard Cell Predicts Emergent Behaviors in Transport, Signaling, and Volume Control. Plant Physiol 159: 1235-1251

6. Clint GM, Blatt MR (1989) Mechanisms of fusicoccin action: evidence for concerted modulations of secondary K^+ transport in a higher-plant cell. Planta 178: 495-508

7. Garcia-Mata C, Gay R, Sokolovski S, Hills A, Lamattina L, Blatt MR (2003) Nitric oxide regulates K^+ and Cl^- channels in guard cells through a subset of abscisic acid-evoked signaling pathways. Proc Natl Acad Sci USA 100: 11116-11121

8. Gilroy S, Fricker MD, Read ND, Trewavas AJ (1991) Role of calcium in signal transduction of Commelina guard cells. Plant Cell 3: 333-344

9. Gorton HL, Williams WE, Assmann SM (1993) Circadian rhythms in stomatal responsiveness to red and blue light. Plant Physiol 103: 399-406

10. Grabov A, Blatt MR (1997) Parallel control of the inward-rectifier K^+ channel by cytosolic-free Ca^{2+} and pH in *Vicia* guard cells. Planta 201: 84-95

11. Grabov A, Blatt MR (1998) Membrane voltage initiates Ca^{2+} waves and potentiates Ca^{2+} increases with abscisic acid in stomatal guard cells. Proc Natl Acad Sci USA 95: 4778-4783

12. Grabov A, Blatt MR (1999) A steep dependence of inward-rectifying potassium channels on cytosolic free calcium concentration increase evoked by hyperpolarization in guard cells. Plant Physiol 119: 277-287

13. Gradmann D, Blatt MR, Thiel G (1993) Electrocoupling of ion transporters in plants. J Membr Biol 136: 327-332

14. Hills A, Chen ZH, Amtmann A, Blatt MR, Lew VL (2012) OnGuard, a Computational Platform for Quantitative Kinetic Modeling of Guard Cell Physiology. Plant Physiol 159: 1026-1042

15. Irving HR, Gehring CA, Parish RW (1992) Changes in cytosolic pH and calcium of guard

cells precede stomatal movements. Proc Natl Acad Sci USA 89: 1790-1794

16. Kinoshita T, Nishimura M, Shimazaki KI (1995) Cytosolic concentration of Ca2+ regulates the plasma membrane H^+- ATPase in guard cells of fava bean. Plant Cell 7: 1333-1342

17. Martinoia E, Maeshima M, Neuhaus HE (2007) Vacuolar transporters and their essential role in plant metabolism. J Exp Bot 58: 83-102

18. McAinsh MR, Brownlee C, Hetherington AM (1991) Partial inhibition of ABA-induced stomatal closure by calcium- channel blockers. Proc R Soc Lond Ser B Biol Sci 243: 195-202

19. McAinsh MR, Brownlee C, Hetherington AM (1992) Visualizing changes in cytosolic-free Ca^{2+} during the response of stomatal guard cells to abscisic acid. Plant Cell 4: 1113-1122

20. McAinsh MR, Pittman JK (2009) Shaping the calcium signature. New Phytol 181: 275-294

21. McClure PR, Shaff JE, Spanswick RM, Kochian LV (1989) Response of the membrane potential of maize roots to nitrate Plant Physiol 89: S-45

22. Meidner H, Willmer CM (1993) Circadian rhythm of stomatal movements in epidermal strips. J Exp Bot 44: 1649-1652

23. Outlaw WHJ (1990) Kinetic properties of guard-cell phosphoenolpyruvate carboxylase. Biochem Physiol Pflanzen 186: 317-326

24. Raschke K (1979) Movements of stomata. In W Haupt, ME Feinleib, eds, Encyclopedia of Plant Physiology, N.S. Vol. 7, Ed 1. Springer, Berlin, pp 373-441

25. Raschke K, Schnabl H (1978) Availability of chloride affects balance between potassium chloride and potassium malate in guard cells of Vicia faba L. Plant Physiol 62: 84-87

26. Rea PA, Poole RJ (1993) Vacuolar H^+-translocating pyrophosphatase. Ann Rev Plant Physiol Mol Biol 44: 157-180

27. Sanders D, Pelloux J, Brownlee C, Harper JF (2002) Calcium at the crossroads of signaling. Plant Cell 14: S401-S417

28. Spanswick RM (1981) Electrogenic ion pumps. Ann Rev Plant Physiol Mol Biol 32: 267-281

29. Staxen I, Pical C, Montgomery LT, Gray JE, Hetherington AM, McAinsh MR (1999) Abscisic acid induces oscillations in guard-cell cytosolic free calcium that involve phosphoinositide-specific phospholipase C. Proc Natl Acad Sci USA 96: 1779-1784

30. Talbott LD, Zeiger E (1993) Sugar and organic acid accumulation in guard cells of *Vicia faba* in response to red and blue light. Plant Physiol 102: 1163-1169

31. Talbott LD, Zeiger E (1996) Central roles for potassium and sucrose in guard cell osmoregulation. Plant Physiol 111: 1051-1057

32. Thiel G, MacRobbie EAC, Blatt MR (1992) Membrane transport in stomatal guard cells: the importance of voltage control. J Membr Biol 126: 1-18

33. Van Kirk CA, Raschke K (1978) Presence of chloride reduces malate production in epidermis during stomatal opening. Plant Physiol 61: 361-364

34. Wang Y, Papanatsiou M, Eisenach C, Karnik R, Williams M, Hills A, Lew VL, Blatt MR (2012) Systems dynamic modelling of a guard cell Cl^- channel mutant uncovers an emergent homeostatic network regulating stomatal transpiration. Plant Physiol 160: 1956-1972

35. Willmer C, Fricker MD. Stomata. 1996. London, Chapman and Hall.